

NPY and TH innervation in human choroidal whole-mounts

A. Triviño, R. de Hoz, B. Rojas, J.J. Salazar, A.I. Ramirez and J.M. Ramirez

Instituto de Investigaciones Oftalmológicas Ramón Castroviejo, Facultad de Medicina,
Universidad Complutense de Madrid, Madrid, Spain

Summary. To determine the distribution of NPY and TH human choroidal innervation, choroidal whole-mounts were processed for indirect immunofluorescence. An antibody to a component of the neuronal cytoskeleton, neurofilament 200 kDa (NF-200) was used to identify neurons and axons. A double immunostaining was performed, antibodies against NF-200 being combined with antibodies against neuropeptide Y (NPY) and tyroxine hydroxylase (TH). Fibers containing both NPY and TH were distributed in three plexuses, one in the suprachoroid large-sized vessel layer, and two in the medium-sized vessel layer. Intrinsic choroidal neurons (ICNs) containing NPY and TH were observed in the suprachoroid. The TH(+) ICNs were located in the medium-sized vessel layer. Overall, NPY(+) and TH(+) ICNs were more frequent in the central temporal area, both in isolation and forming microganglia. We also detected small spindle elements intensely immunoreactive to TH(+) and distributed mainly in the suprachoroid from the equator to the periphery. In conclusion, the human choroid contains abundant NPY and TH nerve fibers related to choroidal vascular structures; it further possesses NPY(+) and TH(+) ICNs which contribute to the choroidal self-regulation persisting after sympathetic denervation. Additionally, these ICNs may at least partially explain why the choroidal blood flow does not respond to the factors that influence systemic vascular control. The preferential location of these cells in the submacular area suggests that dysfunction or degeneration of these cells may be a factor in vascular pathologies found in ocular disease, such as diabetic macular edema or age-related macular degeneration.

Key words: Choroid, Ganglion cells, Innervation, Tyroxine hydroxylase, NPY

Introduction

Choroidal blood flow is thought to be regulated by the autonomic nervous system (Bill, 1975; Koss, 1994) and possibly also by self-regulatory mechanisms (Kiel and Shepard, 1992; Kiel, 1994; Kiel and Van Heuven, 1995). Such self-regulation could explain the weak effect on the fall in choroidal blood flow reported after sympathetic denervation (Bill, 1962, 1984; Alm and Bill, 1970, 1972; Alm, 1977). It could also, partly explain why the choroidal blood flow does not respond to the factors that influence systemic vascular control (Okubo et al., 1990; Kiel and Shepard, 1992; Kiel, 1994; Michelson et al., 1994; Lovasik et al., 2003; Fuchsjager-Mayrl et al., 2003).

The presence of NPY fibers in human choroids has been previously studied (Stone, 1986; Triviño et al., 2002; May et al., 2004). NPY(+) fibers, which reach the choroid through the long and short ciliary nerves (Triviño et al., 2002), could perform a vasoconstrictive function, having been observed in association with the choroidal blood vessels (Stone, 1986; Triviño et al., 2002; May et al., 2004). Perivascular axons have also been identified using antibodies to dopamine- β -hydroxylase (DBH) (Chen et al., 1999; May et al., 2004) and tyroxine hydroxylase (TH) (May et al., 2004). Also, a very low number of NPY(+) intrinsic choroidal neurons (ICNs) in humans has recently been reported (May et al., 2004), although TH(+) ICNs have not yet been described.

More comprehensive knowledge of NPY and TH choroidal innervation could elucidate some unexplained aspects of choroidal physiology. With this aim, we performed a double immunolabeling of choroidal whole-mounts. For this, we used antibodies to NPY, a neuropeptide frequently associated with adrenergic fibers (Lundberg et al., 1982; Allen et al., 1983, 1990; Gu et al., 1983; Furness et al., 1983), and antibodies to TH, the rate-limiting enzyme of catecholamine biosynthesis (Kessler, 1985; Salonen et al., 1996; Norevall and Forsgren, 1999; Anderson et al., 2001; Chung and Chung, 2001). These antibodies were

combined with anti-NF200, a marker of the neuronal cytoskeleton in the central and peripheral nervous system (Liem et al., 1981; Yen and Fields, 1981; Ramirez, 1999). We had reported that anti-NF-200 is a good antibody to visualize ICNs in humans (Triviño, 2002). Thus, a double immunolabeling would allow us to identify ICNs (using anti-NF-200) and distinguish which of them are NPY and which are TH. Choroidal whole-mounts provide a three-dimensional view of choroidal innervation, thus obviating the problems associated with tissue sections, in which the view is restricted to limited parts of the choroid.

Materials and methods

Thirteen adult human eyes (age range 30-58 years) with no ocular disease, enucleated about 2-4 hours postmortem for corneal transplantation, were obtained from the Spanish Eye Bank and studied in accordance with the Helsinki Declaration and local regulations for the use of human tissue in research. All donors had given permission to use their tissues for research.

Immunofluorescence method

After enucleation and corneal processing, the eyes were fixed with 4% paraformaldehyde in 0.1M phosphate buffered saline (PBS) pH 7.4 at 4 °C. The lens, vitreous humor and retina were removed after 15 min fixation. The choroids were then removed from the resulting eyecup and placed in the fixing solution for 24 h at 4 °C. Twelve choroids were then incubated free-floating for up to 10-15 days in 2% hydrogen peroxide at 4 °C for depigmentation. One choroid was not depigmented and was therefore directly processed by immunofluorescence.

Double labeling was performed to demonstrate the co-location of neurofilament 200 kDa (NF-200) with NPY (NF-200/NPY) and TH (NF-200/TH) as described elsewhere (Triviño et al., 2002). Choroidal whole-mounts were incubated with the following primary antibodies: NF-200 (clone NE14, Sigma St. Louis, Missouri USA) in a dilution 1/150 plus NPY (raised in rabbit, Sigma St. Louis, Missouri USA) in a dilution 1/500 or TH (raised in rabbit, Chemicon Temecula, CA, USA) in a dilution 1/100. Binding sites of the primary antibodies were visualized after one day of incubation with the corresponding secondary antibodies: goat antimouse antibody conjugated to fluorescein isothiocyanate (FICT) (Chemicon Temecula, CA, USA) diluted 1/100 or goat antirabbit antibody conjugated to Texas-red (Vector Burlingame, CA, USA) diluted 1/50. Negative controls included replacement of primary and secondary antibodies by normal serum from those species in which the primary antibodies were raised.

Documentation

Human choroidal whole-mounts were examined with a fluorescence microscope (Zeiss, Axioplan 2

Imaging Microscope) equipped with a dichroic filter appropriate for fluorescence-emission spectra of fluorescein isothiocyanate (FITC) and Texas red. This microscope is motorized on the x, y, and z axes to allow spatial correlation of the choroidal nerve structures. Each of the nerve structures at the same choroidal location was digitally photographed by the microscope's own automatic system. The relative correlation of the choroidal structures on the z-axis, or the depth, was estimated by extended focus imaging from up to 60 sections at z-increments of 1-2 microns (z-series stacks). Images were processed using the color-combination tool provided by the Metamorph Imaging System computer program version 4.5 (©Universal Imaging Corps) associated with the Axioplan 2 Imaging Microscope (Zeiss).

Assessing ICN density and size

NPY- and TH-positive ICNs were quantified on whole-mounts. ICNs were counted throughout the choroidal whole-mounts using 40x oil immersion. Only choroids exhibiting good staining quality in the whole sample were selected. As a result of this selection, one choroid was considered for the quantitative study of NPY(+) ICNs and three for the quantitative study of TH(+) ICNs. The best of the three was used to assess TH(+) ICN regional distribution. ICN size was calculated with the measuring tool included in the Metamorph Imaging System version 4.5 computer program (©Universal Imaging Corps) in association with an Axioplan 2 Imaging Microscope (Zeiss). The diameter used to estimate ganglion-cell size was the longest distance between opposing cell boundaries when passing through the center of the cell.

Statistical analysis

The data from analysis of ICN size were uploaded to SPSS 11.5 (comprehensive statistical software; SPSS Inc[®]). ANOVA tests were run to analyze the data. Differences were considered significant when $p \leq 0.05$.

Results

Nerve fibers

Suprachoroid

The short and long ciliary nerves and their branches presented both NPY and TH immunoreactive fibers (Fig. 1A). TH(+) fibers were more abundant than NPY(+) fibers in the long ciliary nerves.

Long-tract axons (extending from the optic nerve head to the periphery) exhibited no immunoreactivity to NPY or TH.

Vessel layers

In the large-sized and medium-sized vessel layers,

Human choroidal NPY and TH innervation

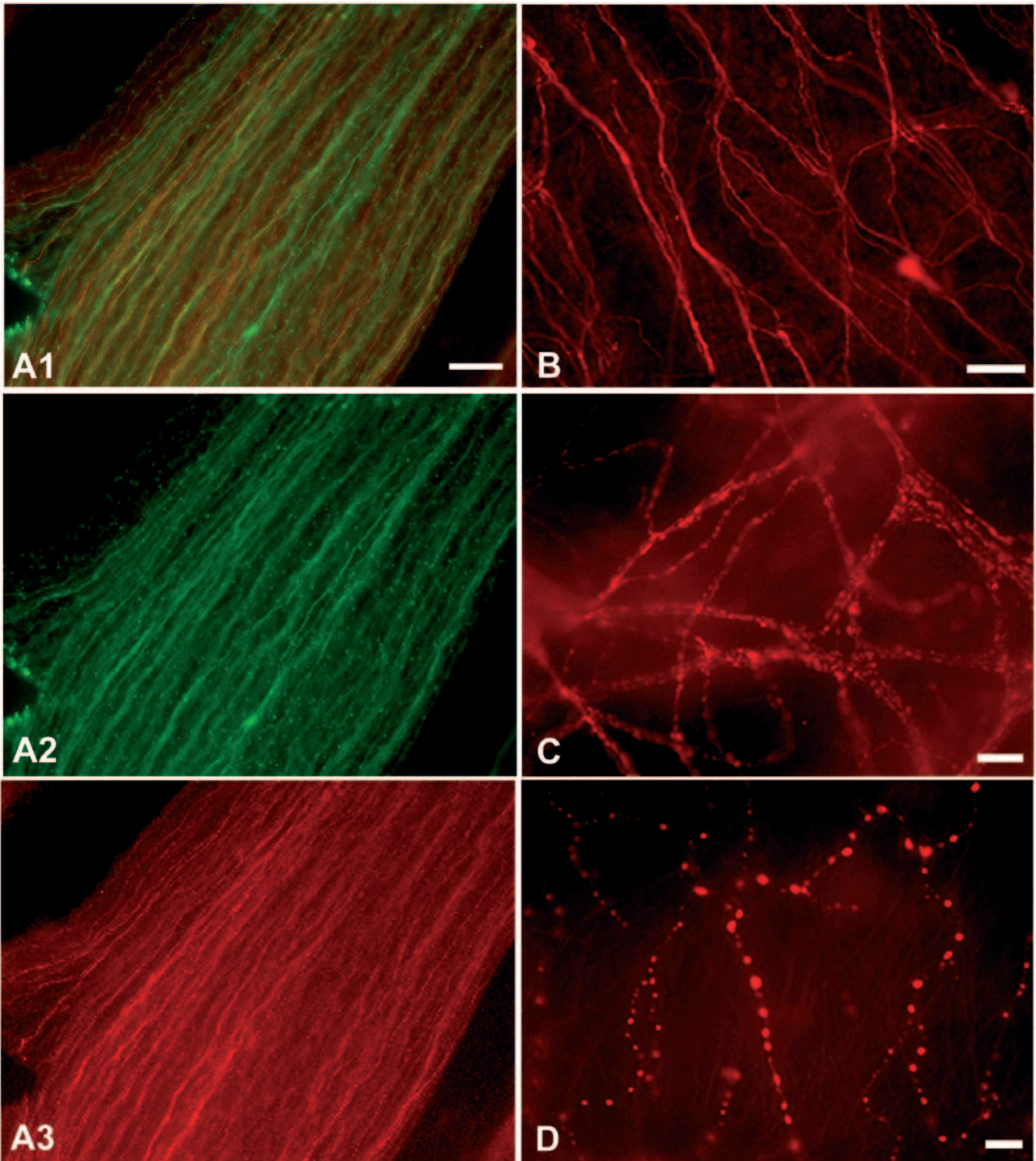


Fig. 1. Immunofluorescence, double immunolabeling for NF-200 (green) and TH (red). **A1-3.** Long ciliary nerve (Bar: 100 μ m). **A1.** Combine double immunostaining. **A2-A3.** For better observation of the structures, the same area marked with each antibody is shown. **A2.** NF-200(+) axons. **A3.** TH(+) axons. **B, C, D.** Nerve fibers at the choroidal vascular layers. **B.** TH(+) axons in large- and medium-sized vessel layers (Bar: 100 μ m). **C.** Thin varicose TH(+) fibers forming a polygonal plexus at the medium-sized vessel layer (Bar: 20 μ m). **D.** The innermost dotted polygonal TH(+) plexus at the medium-sized vessel layer (Bar: 10 μ m).

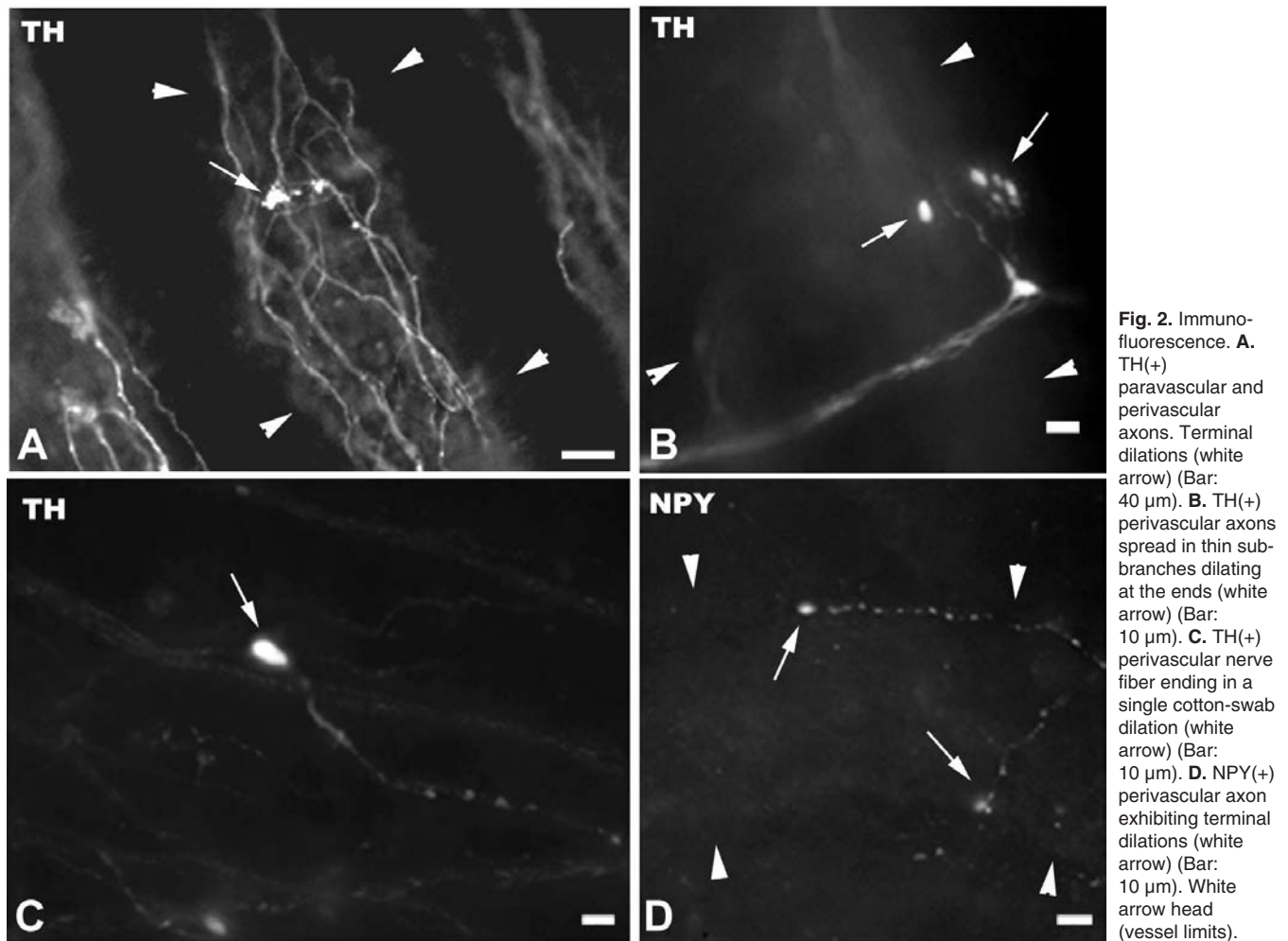
paravascular and perivascular axons were immunoreactive for NPY and TH (Fig. 1B, 2A). On reaching the vessel wall, NPY(+) perivascular axons showed small terminal dilations (Fig. 2D). TH(+) perivascular axons spread out into thin sub-branches, dilating at the ends (Fig. 2B), these dilations varying in morphology (spherical, elliptical). In some instances, the nerve fiber endings close to the vessel wall consisted of a single dilation, presenting a cotton-swab tip shape and intense TH-immunostaining (Fig. 2C). At a deeper level of the medium-sized vessel layer, an additional polygonal plexus was stained for both NPY and TH. This was composed of very thin varicose fibers that formed a mesh throughout the choroid (Fig. 1C). Overall, immunostaining of the 200 kDa neurofilament was difficult to distinguish. At a deeper level of this plexus, a discontinuous polygonal NPY (+) and TH(+) network was also found to extend from the central choroid to the periphery (Fig. 1D). This innermost plexus exhibited no NF-200 immunostaining.

Distribution and characteristics of NP(+) and TH(+) ICNs

Cell counting, distribution and organization

NPY (+) ICN. The NPY(+) ICNs were found only in the suprachoroid, distributed throughout this tissue and in the primary and secondary branches of the short ciliary nerves (Fig. 3A).

We found 112 NPY(+) ICNs (Table 1), all of which had immunostaining for NF-200. These ICNs were examined both in isolation (16%) as well as in groups of 2-9 cells forming microganglia (84%). Most of the microganglia were isolated and some were interconnected (Fig. 3B), although mixed ganglia were also present (only some of the NF-200(+) ICNs were positive for NPY). Overall, NPY(+) ICNs appeared more frequently in the central suprachoroidal area (88.4%) (choroid extending from the optic nerve head to the equator of the eye) than in the periphery (11.6%). NPY(+) ICNs were more numerous in the temporal



Human choroidal NPY and TH innervation

region (63.3%) than in the nasal region (36.7%).

TH(+) ICN. The human choroid contains *TH(+)* ICNs.

The *TH(+)* ICNs found were also *NF-200(+)* and, in contrast to *NPY(+)* ICNS, were located at two different levels: the suprachoroid (Fig. 4A) and the medium-sized

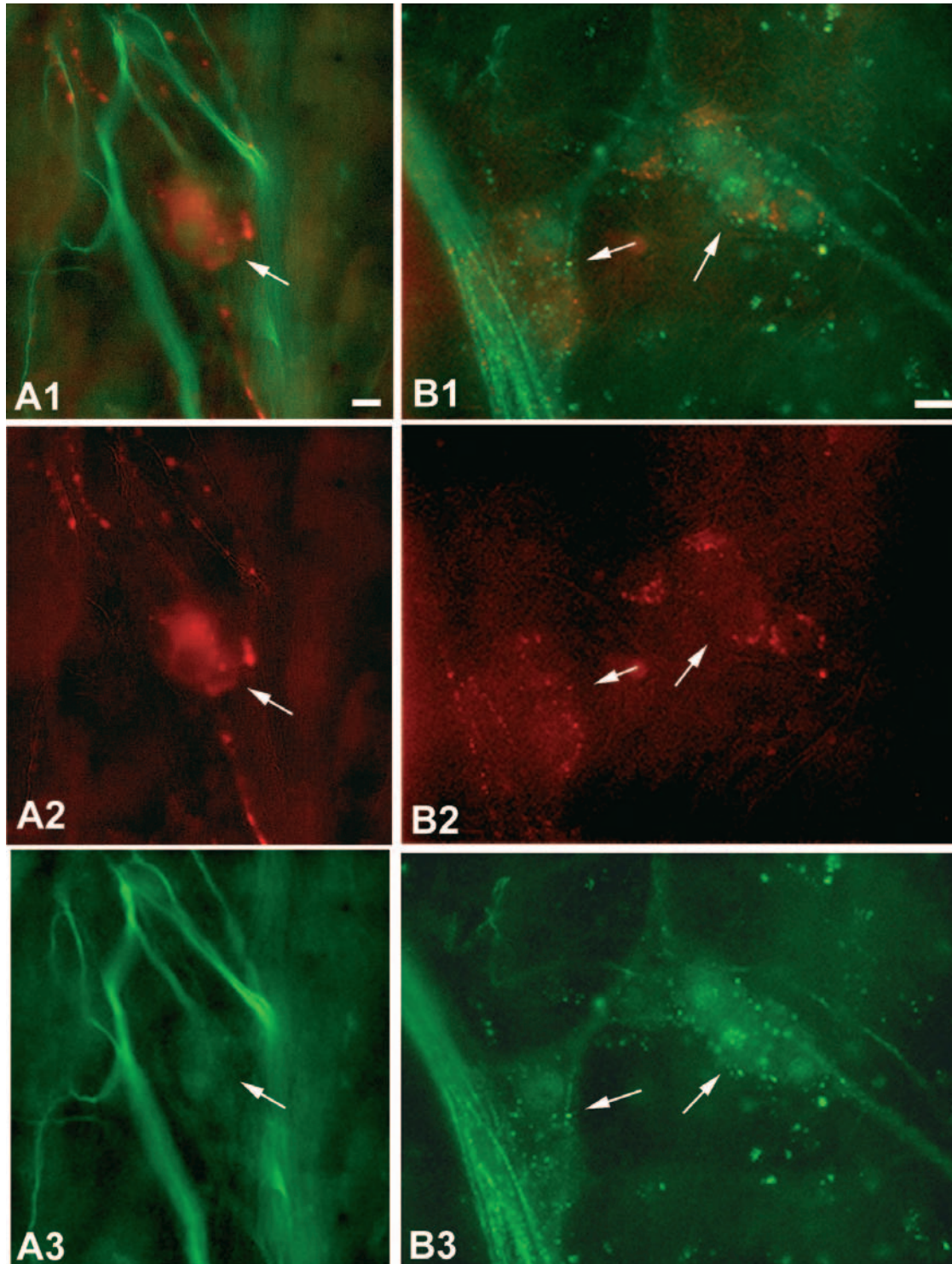


Fig. 3. Immunofluorescence, double immunolabeling for *NF-200* (green) and *NPY* (red). Some figures combine double immunostaining (A1,B1). For better observation of the structures, the same area marked with each antibody is shown (A2-3; B2-3). **A.** *NPY(+)* ICNs in human suprachoroid (white arrow) related with branches of the short ciliary nerves (Bar: 10 μ m). **A2.** ICNs with intense diffuse *NPY* immunopositivity. **B.** *NPY(+)* interconnected microganglia (white arrow) (Bar: 10 μ m).

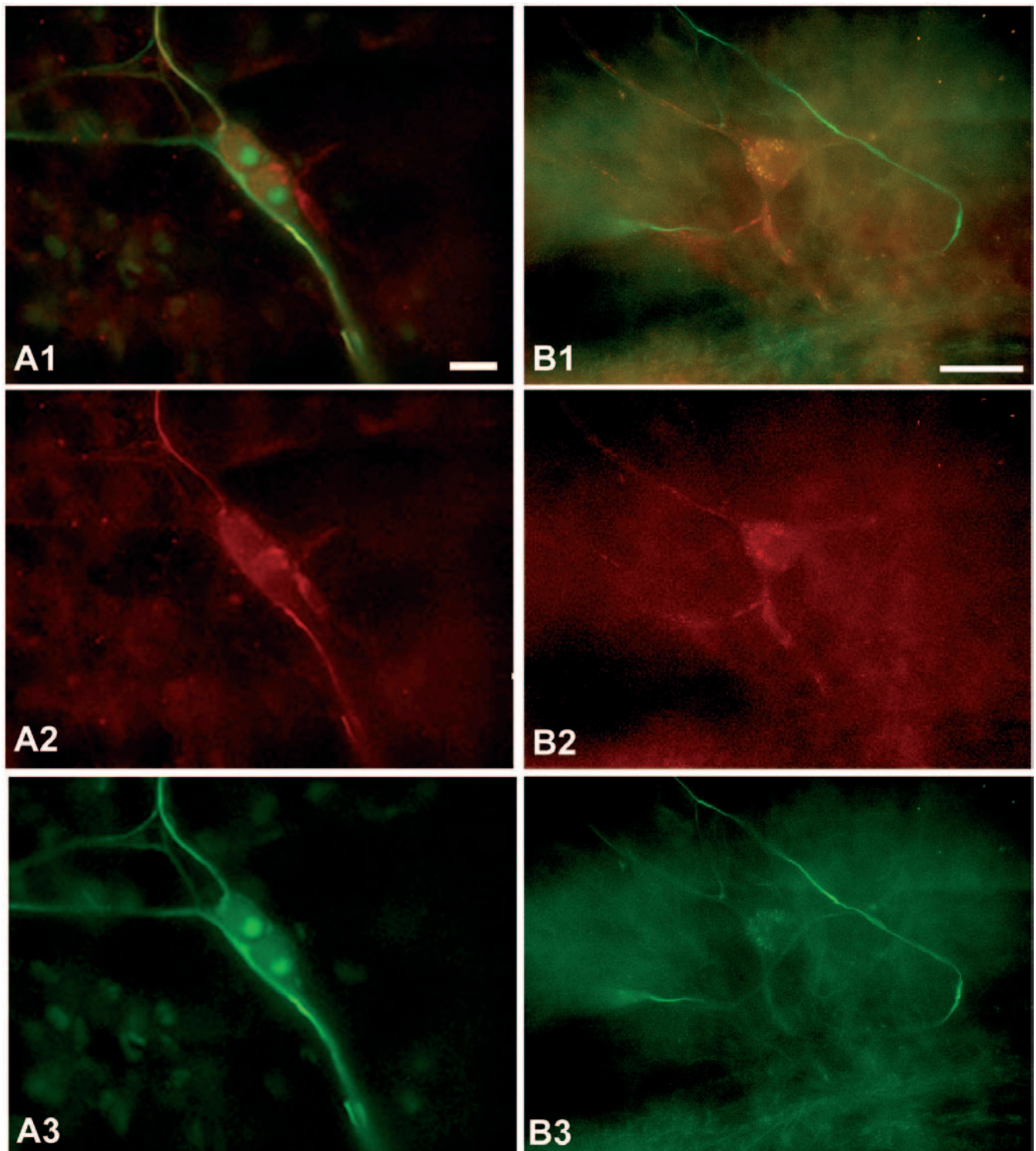


Fig. 4. Immunofluorescence, double immunolabeling for NF-200 (green) and TH (red). Some figures combine double immunostaining (**A1,B1**). For better observation of the structures, the same area marked with each antibody is shown (**A2-3; B2-3**). **A.** Suprachoroidal TH(+) microganglia (Bar: 20 μ m). **A1.** TH(+) ICNs exhibiting diffuse immunostaining. **B.** Multipolar TH(+) ICN at the medium-sized vessel layer (Bar: 40 μ m).

Human choroidal NPY and TH innervation

vessel layer (Figs.4B,5A).

The three tissue samples used to count TH(+) ICNs had 239, 262 and 280, respectively. The choroidal whole-mount used to assess the TH(+) regional distribution contained 262 TH(+) ICNs (Table 2). These were found both in isolation (45.4%) (Fig. 4B, 5A) and in groups of 2-6 cells that formed microganglia (54.6%) (Fig. 4A). Most of the TH(+) ICNs were located in the suprachoroid (92.3%) as well as in the primary and secondary branches of the short ciliary nerves. Of these suprachoroidal TH(+) ICNs, 46.7% were isolated and 53.3% were grouped in microganglia (Fig. 4A). Only a few TH(+) ICNs were found in the medium-sized vessel layer (7.7%): six in isolation (30%) (Fig. 4B,5A) and 14 forming microganglia (70%).

The 242 suprachoroidal TH(+) ICNs were unevenly distributed throughout this layer: 66 % in the central choroidal area, 30% at the equator and 4% in the periphery. Overall, these cells were more numerous in the temporal region (69%) than in the nasal region (31%).

In the medium-sized vessel layer the 20 TH(+) ICNs observed were located in the central area of the temporal region.

Cell morphology and size

The morphology of most of the NPY(+) and TH(+) ICNs was multipolar, with a few bipolar cells. NPY and TH immunopositivity was either diffuse (NPY: Fig.3A , TH: Fig. 4A, 5A) or granular (NPY: Fig. 3B, TH: Fig. 4B).

The NPY(+) ICNs varied in size from 11.79 to 63.29 μ m. Cell size ranged from 18.75-52.53 μ m when isolated (average $37.91 \pm 7.73 \mu$ m) and 11.79-63.29 μ m when grouped in microganglia (average $32.49 \pm 11.63 \mu$ m) ($p < 0.039$). Meanwhile, TH(+) ICNs varied in size from 17.65 to 71.64 μ m diameter. These cells were larger in isolation (average $39.84 \pm 11.09 \mu$ m) than when grouped in microganglia (average $25.92 \pm 4.97 \mu$ m) ($p < 0.000$).

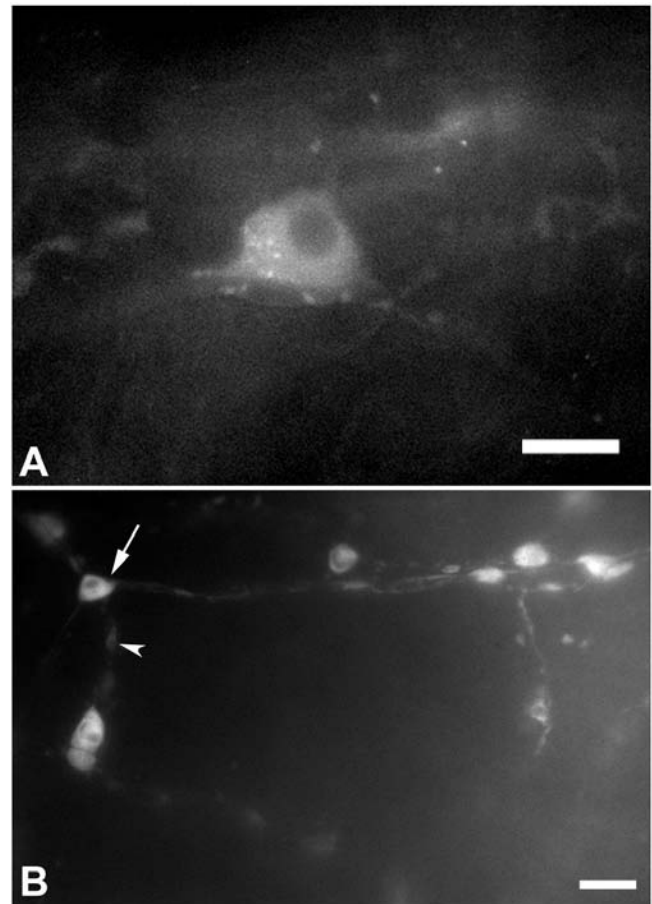


Fig. 5. Immunofluorescence. **A.** TH(+) ICN at the medium-sized vessel layer displaying intense and diffuse immunostaining (Bar: 20 μ m). **B.** TH intensely immunoreactive elements with a circular TH(-) space in their interior (white arrow). Varicose dilation at the fiber bundle (white arrowhead) (Bar: 20 μ m).

Table 1. Distribution of the 112 NPY(+) ICNs.

SUPRACHOROID	ISOLATED ICNs	ICNs IN MICROGANGLIA	CENTRAL CHOROID	PERIPHERAL CHOROID	TEMPORAL CHOROID	NASAL CHOROID
112	18	94	99	13	71	41

Table 2. Distribution of the 262 TH(+) ICNs.

	TOTAL ICNs NUMBER	ISOLATED ICNs	ICNs IN MICROGANGLIA	CENTRAL CHOROID	EQUATORIAL CHOROID	PERIPHERAL CHOROID	TEMPORAL CHOROID	NASAL CHOROID
Suprachoroid	242	113	129	160	72	10	167	75
Medium-size vessel	20	6	14	20	0	0	20	0

Overall, no differences in average size were found between NPY(+) ICNs ($37.91 \pm 7.73 \mu\text{m}$) and TH(+) ICNs ($39.84 \pm 11.09 \mu\text{m}$) when both cell types were in isolation ($p < 0.568$). However, when both were grouped in microganglia, NPY(+) ICNs were significantly larger in size ($32.49 \pm 11.63 \mu\text{m}$) than TH(+) ICNs ($25.92 \pm 4.97 \mu\text{m}$) ($p < 0.006$).

Intensely TH-immunoreactive elements (Fig. 5B)

We detected a population of small spindle elements that were intensely TH(+) and NF-200(-). These elements, which had a circular TH(-) space in the interior, were small in size (ranging from 3.5 mm to 13.3 mm diameter) and ran alongside a TH(+) nerve fiber bundle. This fiber bundle presented large varicose dilations that differed in size and morphology from the intensely TH(+) elements.

We found 172 intensely TH(+) elements throughout the suprachoroid, 83 in the temporal region (48.3%) and 89 in the nasal region (51.7%). Most of these were located at the equator and in the periphery (95.3%). Only 8 intensely TH(+) elements were detected at the posterior pole (4.7%).

Discussion

Both NPY(+) and TH(+) fibers were distributed in three plexuses, one in the suprachoroid –large-sized vessel layer, and two in the medium-sized vessel layer. In the latter layer, the fibers were at different depths. The innermost dotted polygonal NPY(+) or TH(+) plexus exhibited no NF-200 immunostaining. NF immunostaining does not necessarily label all portions of the axons and thus may leave the preterminal part of the axons unstained (Cuthbertson et al., 1997). The innermost plexus observed by us could be the TH(+) plexus reported by May et al. (2004) in choroidal sections at the precapillary arterioles.

Analysis of anti-NPY and anti-TH processed choroids differed with regard to the fibers that reach the vessel walls (perivascular axons) and the ICNs. We found more diversity in perivascular axon endings with anti-TH than with anti-NPY. One of the reasons may be the nature of the antigens analyzed. That is, TH, as the rate-limiting enzyme of catecholamine biosynthesis, has to be synthesized at the terminals. In contrast, NPY is synthesized only in the cell body, where it is packaged in secretory granules and synaptic vesicles, which are transported from the cell body to the terminals (Schwartz, 2000).

Antibodies to NPY and TH stained ICNs at the suprachoroid. However, only anti-TH revealed an additional small group of ICNs (7% of the total TH(+) ICNs observed), which was located in the medium-sized vessel layer. Overall, TH(+) ICNs were more numerous than NPY(+) ICNs. We have previously reported that the human choroid has 1300-1500 neurons (Triviño et al., 2002), and, based on this data, TH(+) ICNs would

represent 17.5-20.2% of such cells, and NPY(+) ICNs 7.5-8.6%. Both NPY(+) and TH(+) ICNs were more frequently found in the central region of the temporal area (the choroid underneath the macular area of the retina). There were no differences in morphology or immunostaining characteristics between the two ICN populations.

Most NPY(+) ICNs were grouped in microganglia. When both types of ICNs were grouped in microganglia, NPY(+) ICNs were in most cases larger than TH(+) ones. The biological significance of these differences in grouping and size between NPY(+) and TH(+) ICNs is unknown and deserves further research.

The NPY(+) ICNs observed in the present work were larger and more numerous than those previously reported (May et al., 2004). The use of whole-mounts could account for the greater number found by us. Additionally, the performance of z-series stacks, as defined in the Methods section, enabled us to measure the maximum diameter of the ICN.

This is the first description available of TH(+) ICNs in humans. A previous report describing intense innervation surrounding half the human ICNs by TH(+) nerve fibers (May et al., 2004) postulated that most of these TH(+) endings originated from the superior cervical ganglion, where most of the neurons stain positively for NPY (Matsumoto et al., 1992), noradrenaline, TH and DBH (Grimes et al., 1998; Tajti et al., 1999). Our findings suggest that some of the TH(+) endings could originate from the TH(+) ICNs observed by us.

The human choroid has also been found to contain small intensely TH(+)/NF-200(-) elements distributed throughout the suprachoroid. Their morphology is reminiscent of the neuron-like cells reported in the primate ovary (Dess, 1995) and of the small intensely fluorescent (SIF) TH(+) cells recently found in the intrinsic cardiac nervous system of the rat (Horackova et al., 2000; Slavikova et al., 2003). Also, consistent with our findings, two types of TH(+) cells (SIF cells and large-diameter neurons) have been described in the intrinsic cardiac nervous system (Horackova et al., 2000; Slavikova et al., 2003).

Functional considerations

The choroidal blood flow is regulated by the autonomic nervous system (Bill, 1975; Koss, 1994), and by a self-regulatory mechanism (Kiel and Shepard, 1992; Kiel, 1994; Kiel and Van Heuven, 1995). In this way, the choroid is able to maintain a constant blood flow over wide swings in main arterial pressure (Okubo et al., 1990; Michelson et al., 1994) or intraocular pressure (Kiel, 1994) as well as under physiological (Lovasik et al., 2003) or pharmacological stimuli (Fuchjager-Mayrl et al., 2003).

The sympathetic innervation of the choroid helps regulate blood flow by means of vasoconstriction (Bill, 1991). This appears to be a protective mechanism to

Human choroidal NPY and TH innervation

prevent over-perfusion and breakdown of barriers (Bill and Linder, 1976). Some studies (Bill, 1962, 1984; Alm and Bill, 1970, 1972; Alm, 1977) have shown that although choroidal vasoconstriction occurs during direct sympathetic stimulation, sympathetic denervation has little effect on the fall in choroidal blood flow during hemorrhagic hypotension. Therefore, the most likely explanation for these results is that the choroid is not a passive agent of circulation but is capable of considerable self-regulation. The NPY(+) and TH(+) ICNs mentioned in the present work could participate in the self-regulatory mechanisms of the choroid that have long been postulated. It has recently been confirmed that the target of the ICNs in the human eye is mainly the choroidal vasculature (Schrödl et al., 2003).

Experimental data have shown that sympathetic innervation is critical in regulating choroidal vascularity, and that chronic loss of sympathetic activity may contribute to abnormal vascular regulation in diseases such as age-related macular degeneration (Smoliakova and Radivoz, 1988; Schmidt et al., 1997) and diabetic macular edema (Ishikawa et al., 1985; Fulk et al., 1991). Sympathetic axonal damage is a noteworthy feature of diabetic neuropathy, and an ocular sympathetic nerve dysfunction in diabetic patients has been suggested (Ernest, 1988). In patients with diabetic macular edema (the main cause of legal blindness in this population) episodes of hyperglycemia may result in increased blood flow and pressure in the submacular choroidal circulation (Ernest, 1988). The NPY(+) and TH(+) ICNs described in the present work were preferentially located in the submacular region. The dysfunction of these ICNs could contribute to diabetic macular edema.

In pathological situations of high intraocular pressure in humans, the blood flow in the submacular choroid is reduced by up to 90% (Riva et al., 1994). Moreover, in primate eyes with primary and secondary glaucoma, the number of ICNs is reduced, particularly in the central choroidal region (May et al., 1997). Thus, neuronal alterations originating in the submacular region could be involved in microcirculatory changes that produce hypoperfusion in glaucoma and other pathologies.

In conclusion, the plexuses containing NPY and TH fibers could contribute to blood-flow regulation in the submacular area. This vascular control could be explained by the presence of neurotransmitters on perivascular and paravascular axons, with proven effects on vascular regulation and on ICNs.

Acknowledgments. This research was supported by the Ministerio de Ciencia y Tecnología, Plan Nacional de Investigación Científica, Desarrollo e Innovación Tecnológica (Grant BFI03-08108) of Spain.

References

Alm A. (1977). The effect of sympathetic stimulation on blood flow through the uvea, retina and optic nerve in monkeys (*Macaca irus*).

- Exp. Eye. Res. 25,19-24.
- Alm A. and Bill A. (1970). Blood flow and oxygen extraction in the cat uvea at normal and high intraocular pressures. *Acta. Physiol. Scand* 80, 19-28.
- Alm A. and Bill A. (1972). The oxygen supply to the retina: II. Effects of high intraocular pressure and of increased arterial carbon dioxide tension on uveal and retinal blood flow in cats: a study with radioactively labelled microspheres including flow determinations in brain and some other tissues. *Acta. Physiol. Scand.* 84, 306-319.
- Allen J.M., McGregor G.P., Adrian T.E., Bloom S.R., Zhang S.Q., Ennis K.W. and Unger W.G. (1983) Reduction of neuropeptide Y (NPY) in the rabbit iris-ciliary body after chronic sympathectomy. *Exp. Eye.Res.* 37, 213-215.
- Allen J.M., Rodrigo J., Kerle D.J., Darcy K., Williams G., Polak J.M. and Bloom S.R. (1990). Neuropeptide Y (NPY)-containing nerves in mammalian ureter. *Urology* 35, 81-86.
- Anderson R.L., Morris J.L. and Gibbins I.L. (2001). Neurochemical differentiation of functionally distinct populations of autonomic neurons. *J. Comp. Neurol.* 429, 419-435.
- Bill A. (1962). Autonomic nervous control on uveal blood flow. *Acta Physiol. Scand.* 56, 70-81.
- Bill A. (1975). Blood circulation and fluid dynamics in the eye. *Physiol. Rev.* 55, 383-417.
- Bill A. (1984). Effects of acute hemorrhaging on the blood flow in the eye and some other tissues in the rabbit: role of sympathetic nerves. *Klin. Monatsbl. Augenheilkd.* 184, 305-307.
- Bill A. (1991). Effects of some neuropeptides on the uvea. *Exp. Eye Res.* 53, 3-11.
- Bill A. and Linder J. (1976). Sympathetic control of cerebral blood flow in acute arterial hypertension. *Acta Physiol. Scand.* 96, 114-121.
- Chen Z., Gia W., Kaufman P.L. and Zynader M. (1999). Immunohistochemical localization of dopamine-beta-hydroxylase in human and monkey eyes. *Curr. Eye Res.* 18, 39-48.
- Chung K. and Chung J.M. (2001). Sympathetic sprouting in the dorsal root ganglion after spinal nerve ligation: evidence of regenerative collateral sprouting. *Brain Res.* 859, 204-212.
- Cuthbertson S., Jackson B., Toledo C., Fitzgerald M.E.C., Shih Y.F., Zagvazdin Y.S. and Reiner A. (1997). Innervation of orbital and choroidal blood vessels by the pterygopalatine ganglion in pigeons. *J. Comp. Neurol.* 386, 422-442.
- Dees W.L., Hynai J.K., Schultea T.D., Mayerhofer A., Danilchik M., Dissen G.A. and Ojeda S.R. (1995). The primate ovary contains a population of catecholaminergic neuron-like cells expressing nerve growth factor receptors. *Endocrinology* 136, 5760-5768.
- Ernest J. (1988). Regulatory mechanism of the choroidal vasculature in health and disease. In: *Retinal diseases: biomedical foundations and clinical management.* Tso M.O.M. (ed). JB Lippincott. Philadelphia. pp 125-130.
- Fuchsjager-Mayrl G., Malec M., Amoako-Mensah T., Kolojaschna J. and Schmetterer L. (2003). Changes in choroidal blood-flow during light-dark transitions are not altered by atropine or propranolol in healthy subjects. *Vis. Res.* 43, 2185-2190.
- Fulk G.W., Bower A., McBride K. and Boatright R. (1991). Sympathetic denervation of the iris dilator in noninsulin-dependent diabetes. *Optom. Vis. Sci.* 68, 954-956.
- Furness J.B., Costa M., Emson P.C., Hakanson R., Moghimzadeh E., Sundler F., Taylor I.L. and Chance R.E. (1983) Distribution, pathways and reactions to drug treatment of nerves with neuropeptide Y- and pancreatic polypeptide-like immunoreactivity in

- the guinea-pig digestive tract. *Cell. Tissue Res.* 234, 71-92.
- Grimes P.A., Koeberlein B., Tigges M. and Stone R.A. (1998). Neuropeptide Y-like immunoreactivity localizes to preganglionic axons terminals in the rhesus monkey ciliary ganglion. *Invest. Ophthalmol. Vis. Sci.* 39, 227-232.
- Gu J., Polak J.M., Allen L.M., Huang W.M., Sheppard M.N., Tatemoto K. and Bloom S.R. (1984) High concentration of a novel peptide, neuropeptide Y, in the innervation of mouse and rat head. *J. Histochem. Cytochem.* 32, 467-472.
- Horakova M., Slavikova J. and Byczko Z. (2000). Postnatal development of the rat intrinsic cardiac nervous system: a confocal laser scanning microscopy study in whole-mount atria. *Tissue Cell* 32, 377-388.
- Ishikawa S., Bensaoula T., Uga S. and Mukuno K. (1985). Electron-microscopic study of iris nerves and muscles in diabetes. *Ophthalmologica* 191, 172-183.
- Kessler J.A. (1985). Parasympathetic, sympathetic, and sensory interactions in the iris: nerve growth factor regulates cholinergic ciliary ganglion innervation in vivo. *J. Neurosci.* 5, 2719-2725.
- Kiel J.W. (1994). Choroidal myogenic autoregulation and intraocular pressure. *Exp. Eye Res.* 58, 529-543.
- Kiel J.W. and Shepard A.P. (1992). Autoregulation of choroidal blood flow in the rabbit. *Invest. Ophthalmol. Vis. Sci.* 33, 2399-2410.
- Kiel J.W. and Van Heuven W.A.J. (1995). Ocular perfusion pressure and choroidal blood flow in the rabbit. *Invest. Ophthalmol. Vis. Sci.* 36, 579-585.
- Koss M.C. (1994). Adrenoceptor mechanisms in epinephrine induced anterior choroidal vasoconstriction in cats. *Exp. Eye Res.* 59, 715-722.
- Liem R.K.H., Keith C.H., Leterrier J.F., Trenckner E., Shelanski M.L. (1981). Chemistry and biology of neuronal and glial intermediate filaments. *Col. Spring. Harb. Symp. Quant. Biol.* 46, 341-350.
- Lovasik J.V., Kergoat H., Riva C.E., Petrig B.L. and Geiser M. (2003). Choroidal blood-flow during exercise-induced changes in the ocular perfusion pressure. *Invest. Ophthalmol. Vis. Sci.* 44, 21326-2132.
- Lundberg J.M., Terenius L., Hökfelt T., Martlin C.R., Tatemoto K., Mutt V., Polak J., Bloom S. and Goldstein M. (1982). Neuropeptide Y (NPY)-like immunoreactivity in peripheral noradrenergic neurons and effects of NPY on sympathetic functions. *Acta Physiol. Scand.* 116, 477-480.
- Matsumoto Y., Tanabe T., Ueda S. and Kawata M (1992). Immunohistochemical and enzyme histochemical studies of peptidergic, aminergic and cholinergic innervation of the lacrimal gland of the monkey (*Macaca fuscata*). *J. Auton. Nerv. Syst.* 37, 207-214.
- May C.A., Hayreh S.S., Furuyoshi N., Ossoinig K., Kaufman P.L. and Lütjen-Drecoll E. (1997). Choroidal ganglion cell plexus and retinal vasculature in monkeys with laser-induced glaucoma. *Ophthalmologica* 211, 161-171.
- May C.A., Neuhuber W. and Lütjen-Drecoll E. (2004). Immunohistochemical classification and functional morphology of human choroidal ganglion cells. *Invest. Ophthalmol. Vis. Sci.* 44, 361-367.
- Michelson G., Groh M. and Gründler A. (1994). Regulation of ocular blood flow during increases of arterial blood pressure. *Br. J. Ophthalmol.* 78, 461-465.
- Norevall L.I. and Forsgren S. (1999). NPY/ sympathetic and NPY/VIP innervation of the blood vessels supplying rat tooth-related structures: effects of sympathectomy. *Neuropeptides* 33, 216-226.
- Okubo H., Gherezghiher T. and Koss M.C. (1990). Long posterior ciliary arterial blood flow an systemic blood pressure. *Invest. Ophthalmol. Vis. Sci.* 31, 819-826.
- Ramirez J.M., Triviño A., De Hoz R., Ramirez A.I., Salazar J.J. and García Sánchez J. (1999). Immunohistochemical study of rabbit choroidal innervation. *Vis. Res.* 39, 1246-1262.
- Riva C.E., Cranstoun S.D., Grunwald J.E. and Petrig B.L. (1994). Choroidal blood flow in the foveal region of the human ocular fundus. *Invest. Ophthalmol. Vis. Sci.* 35, 4273-4281.
- Salonen T., Haapalinna A., Heinonen E., Suhonen J. and Hervonen A. (1996). Monoamine oxidase B inhibitor seligiline protects young and aged rat peripheral sympathetic neurons against 6-hydroxydopamine-induced neurotoxicity. *Acta. Neuropathol. (Berl)* 91, 466-474
- Schrödl F., De Laet A., Tassignon M.J., Van Bogaert P.P., Brehmer A., Neuhuber W. and Timmermans J.P. (2003). Intrinsic choroidal neurons in the human eye: projections, targets and basic electrophysiological data. *Invest. Ophthalmol. Vis. Sci.* 44, 3705-3712.
- Slavikova J., Kuncova J., Reischig J. and Dvorakova M. (2003). Catecholaminergic neurons in the rat intrinsic cardiac nervous system. *Neurochem. Res.* 28, 593-598.
- Schmidt R.E., Beaudet L.N., Plurad S.B. and Dorsey D.A. (1997). Axonal cytoskeletal pathology in aged and diabetic human sympathetic autonomic ganglia. *Brain. Res.* 769, 375-383.
- Schwartz J.H. (2000). Neurotransmitter. In: Principles of neural science. Kandel E. R., Schwartz J.H. and Jessell T.M. (eds). McGraw-Hill Companies. New York. pp 280-297.
- Smoliakova G.P. and Radivoz M.I. (1988). Morphological retinal changes in experimental disorders of the sympathetico-adrenal system. *Vestn. Oftalmol.* 104, 58-61.
- Stone R.A. (1986). Neuropeptide Y and innervation of the human eye. *Exp. Eye Res.* 42, 349-355.
- Tajti J., Moller S., Uddman R., Bodi I. and Edvinsson L. (1999). The human superior cervical ganglion: neuropeptides and peptides receptors. *Neurosci. Lett.* 263, 121-124.
- Triviño A., De Hoz R., Salazar J.J., Ramirez A.I., Rojas B. and Ramirez J.M. (2002). Distribution and organization of the nerve fibers and ganglion cells of the human choroids. *Anat. Embryol.* 205, 417-430.
- Yen S.H. and Fields K.L. (1981). Antibodies to neurofilament, glial filament, and fibroblast intermediate filament protein, being to different cell types of the nervous system. *J. Cell Biol.* 88, 115-126.